

# Simple Radiology VLLM Test-time Scaling with Thought Graph Traversal

Yue Yao<sup>\*</sup>, Zelin Wen<sup>\*</sup>, Yan Tong<sup>\*</sup>, Xinyu Tian,  
Xuqing Li, Xiao Ma, Dongliang Xu<sup>†</sup>, Tom Gedeon

<sup>a</sup>Shandong University, No. 17923 Jingshi Road, Jinan, 250061, Shandong, China

<sup>b</sup>Australian National University, Acton Campus, Canberra, 2601, ACT, Australia

<sup>c</sup>Curtin University, Kent Street, Perth, 6102, Western Australia, Australia

---

## Abstract

Test-time scaling offers a promising way to improve the reasoning performance of vision-language large models (VLLMs) without additional training. In this paper, we explore a simple but effective approach for applying test-time scaling to radiology report generation. Specifically, we introduce a lightweight Thought Graph Traversal (TGT) framework that guides the model to reason through organ-specific findings in a medically coherent order. This framework integrates structured medical priors into the prompt, enabling deeper and more logical analysis with no changes to the underlying model. To further enhance reasoning depth, we apply a reasoning budget forcing strategy that adjusts the model’s inference depth at test time by dynamically extending its generation process. This simple yet powerful combination allows a frozen radiology VLLM to self-correct and generate more accurate, consistent chest X-ray reports. Our method outperforms baseline prompting approaches on standard benchmarks, and also reveals dataset biases through traceable reasoning paths. Code and prompts are open-sourced for reproducibility at <https://github.com/glerium/Thought-Graph-Traversal>.

**Keywords:** Vision-language large models, Chest X-ray reports generation, Test-time scaling

---

## 1. Introduction

Performance gains in vision-language large models in recent years have predominantly stemmed from increasing training-time computational resources, particularly through the collection of large-scale datasets for self-supervised pretraining [1]. These advancements have enabled a shift toward a new paradigm: *test-time scaling*, which focuses on enhancing model performance by increasing computation during inference [2, 3, 4]. A growing body of work like Snell *et al.* has explored this concept [5],

---

<sup>1</sup> <sup>\*</sup>Equal contribution.

<sup>2</sup> <sup>†</sup> Corresponding author.

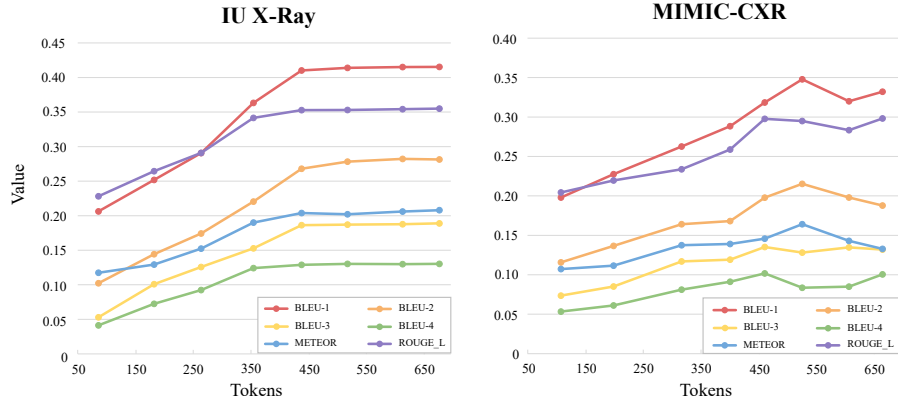


Figure 1: **Test-time scaling with Thought Graph Traversal.** We apply test-time scaling to radiology report generation by introducing a Thought Graph Traversal framework, which enables structured, multi-step reasoning under varying test-time compute budgets. Our method improves report quality when reasoning budget increase (measured by the length of reasoning tokens). Notably, model accuracy shows a positive correlation with the number of reasoning tokens used during inference, until it reaches a saturation point beyond which additional reasoning yields diminishing returns.

and its effectiveness was recently confirmed by OpenAI’s o1 [6], which achieved notable reasoning improvements by scaling test-time compute. OpenAI attributes this to large-scale reinforcement learning (RL), which implies extensive use of data [6]. In response, various groups have attempted to replicate the success of o1 using strategies like Monte Carlo Tree Search [7], multi-agent collaboration [8], and other techniques like multi-stage reinforcement learning in DeepSeek R1 [9]. Nevertheless, a task specific implementation of test-time scaling in a specific area (*i.e.*, medical report generation) has yet widely studied.

Our approach is also motivated by recent research in medical report generation. Many existing methods like Chen *et al.* employ encoder-decoder architectures [10]. These methods aim to produce complete radiology reports from input images. However, several critical shortcomings remain unaddressed. **Structural Deficiency:** many generated radiology reports lack standardized structure, reducing readability and making it harder for clinicians to identify essential findings [11]. This issue is exacerbated by training on datasets composed of inconsistent and heterogeneous report formats. As a result, uniformity and clarity in generated outputs are compromised. **Lack of Interpretability and Interactivity:** Current systems often fail to provide transparent reasoning, relying instead on attention maps that offer limited insights. Furthermore, they lack mechanisms for clinicians to guide or modify the report generation process in accordance with specific patient contexts. This lack of transparency and flexibility limits their usefulness in real-world settings [12].

Addressing these limitations, we propose a Thought Graph Traversal (TGT) that explicitly manages the depth of reasoning within VLLMs during inference. By integrating a dedicated reasoning mechanism, our model dynamically controls the extent of logical reasoning at test time, enabling deeper and more clinically relevant analy-

ses. Additionally, Thought Graph Traversal allows structured prior medical knowledge, systematically guiding the model towards logically coherent and medically accurate outputs. We conduct extensive ablation experiments targeting the structured reasoning of VLLMs’ results. An additional benefit of this module is its capacity to expose underlying biases present in chest X-ray datasets, which is crucial for improving model generalizability and fairness.

Through extensive experimentation, our method demonstrates superior performance compared to baseline models across established benchmark datasets (*e.g.*, MIMIC-CXR). Shown in Figure 1, by implementing reasoning budget forcing, we successfully scale the model’s inference capabilities, resulting in significant improvements in diagnostic accuracy of generated reports. To foster transparency, reproducibility, and community-driven advancements, our developed model, along with datasets and source code, are publicly available.

## 2. Related work

**Vision Large Language Model.** Recent advances in Transformer and computing have enabled very large language models (LLMs) like ChatGPT [13] with enhanced performance on text generation and translation. Architectures like CLIP [14] achieve multimodal understanding via image-text pretraining. Additionally, recent work guides LLMs via prompts rather than explicit training. For example, VisualChatGPT [15] connects ChatGPT with vision models for image-inclusive conversations, exemplifying this more flexible prompt-based approach to unleashing LLM potential. The idea of guiding LLMs through prompts has inspired our research. Guiding an LLM through anatomical region prompts results in structured, interpretable reports. Furthermore, clinical context prompts facilitate physician interactivity, enhancing the practical utility of the generated reports.

**Radiology VLLMs.** Recent frameworks like Wang *et al.* build on medical image captioning to incorporate expert or external knowledge for richer contextual understanding in generated radiology reports [16]. Recent approaches like the MET [16], Kiut [16], and KBMA [17] incorporate specialized knowledge through fusion of expert tokens, multimodal injection, and trainable knowledge bases to enhance contextual understanding in radiology report generation. The work [18] uses anatomical regions for the first time to generate reports. To further increase interpretability, some efforts like Qin *et al.* introduce memory networks [19] to store knowledge and learn implicit image-text links. Unlike these methods focusing on model training, we focus on model test-time scaling only.

**Knowledge graphs** have been widely used to incorporate domain knowledge for assisting radiology report generation. For example, [20] proposed integrating pre-constructed graphs that capture relationships between diseases and organs via graph neural networks, enabling dedicated abnormality-aware feature learning. [21] later extended this idea by dynamically updating the graph with new knowledge during training. More recently, [22] designed a knowledge distillation module that fuses information from a symptom graph into the final decoding stage, which shares conceptual similarities with the dynamic decision prompting (DDP) in our work. However, all these approaches rely on modifying the model through training or finetuning. In contrast, our method

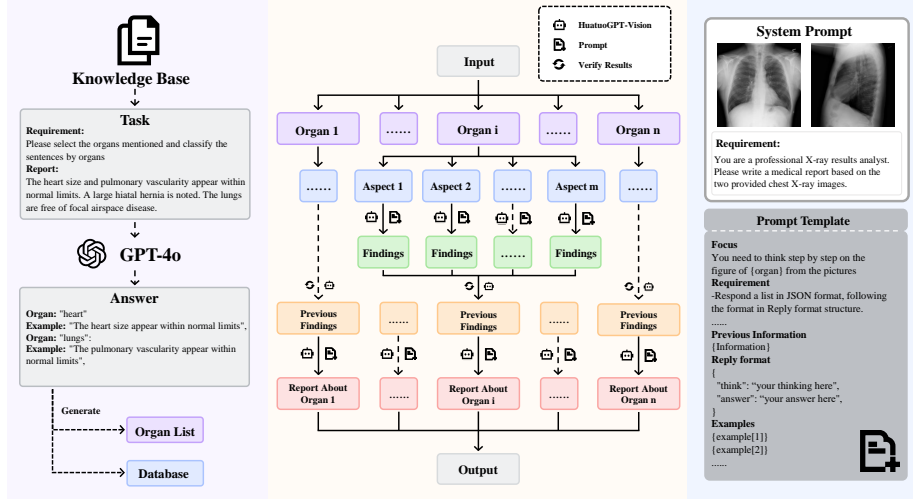


Figure 2: **Overview of Thought Graph Traversal for structured radiology report generation.** (Left) In the preprocessing stage, GPT-4o is used to extract organ entities and their corresponding descriptions from training reports, which are stored in `organ_list` and `database`. (Center) During inference, for each patient, a fixed set of questions is asked per organ (orange boxes), generating diverse viewpoints on an organ independently. These intermediate answers are then aggregated in the final stage (red box), where the VLLM integrates all information to generate an organ-specific statement using in-context examples. (Right) Prompt templates are dynamically filled with organ names, retrieved expert examples, and question-answer pairs. The final report is produced by concatenating the generated statements in a logical order across organs.

performs test-time scaling only, leaving the VLLM architecture and weights untouched. We use a structured prompting mechanism based on a Thought Graph Traversal, which guides the model’s reasoning process in a lightweight and plug-and-play fashion. Despite its simplicity, our method achieves stronger clinical efficacy without requiring additional training or parameter updates.

**Prompt engineering and test time scaling.** Prompt engineering usually integrates human-like problem-solving knowledge [2]. For example, few-shot prompting [23] allows language models (LMs) to generate responses by providing them with explicit examples. The chain-of-thought (CoT) method [24], along with its variants such as zero-shot CoT [25], graph-of-thought (GoT) [26, 27], and tree-of-thought (ToT) [28], intricately designs prompts to emulate various types of human-like reasoning processes. Some other works like Gou *et al.* [29] manually craft prompts that encourage LLMs to engage in critical thinking and verification processes before delivering the final answer. Recent works begin to use prompt engineering for achieving test time scaling [2]. However, they focus on general methods without a design for a domain-specific area like medical report generation. We, for the first time, design a test time scaling (*i.e.*, TGT) framework for radiology VLLM.

### 3. Method

#### 3.1. Recap of Radiology VLLM

We define the medical report generation task as a conditional sequence generation problem. Given a chest X-ray image  $\mathbf{x}$ , the model is required to generate a textual report  $\mathbf{y} = (y_1, y_2, \dots, y_T)$ , where  $y_t$  denotes the  $t$ -th token in the output sequence. Formally,

$$\hat{\mathbf{y}} = \arg \max_{\mathbf{y}} P(\mathbf{y}|\mathbf{x}; \theta), \quad (1)$$

where  $\theta$  are the model parameters. Recent radiology VLLM approaches often adopt encoder-decoder architectures: **Visual Encoder**  $f_v$ : A CNN or vision transformer (ViT) extracts image features  $\mathbf{z}_v = f_v(\mathbf{x})$ . **Language Decoder**  $f_l$ : A Transformer-based decoder generates the report conditioned on  $\mathbf{z}_v$ . Despite their success, these models face two key limitations:

- **Unstructured Output:** Reports  $\mathbf{y}$  generated from heterogeneous training sets lack a standardized format, reducing clinical clarity.
- **Weak Reasoning:** Existing models optimize log-likelihood over  $P(\mathbf{y}|\mathbf{x})$ , but lack mechanisms to perform structured or multi-step reasoning.

While these prior radiology-focused vision-language models (VLLMs) adopt encoder-decoder architectures to generate reports from medical images, these models are typically fine-tuned on narrow domain-specific corpora and lack the flexibility to follow complex textual prompts. Their decoding process is often rigid and solely optimized for next-token prediction, which limits their capacity for test-time control or explicit reasoning. Moreover, due to the lack of native instruction-following capabilities and

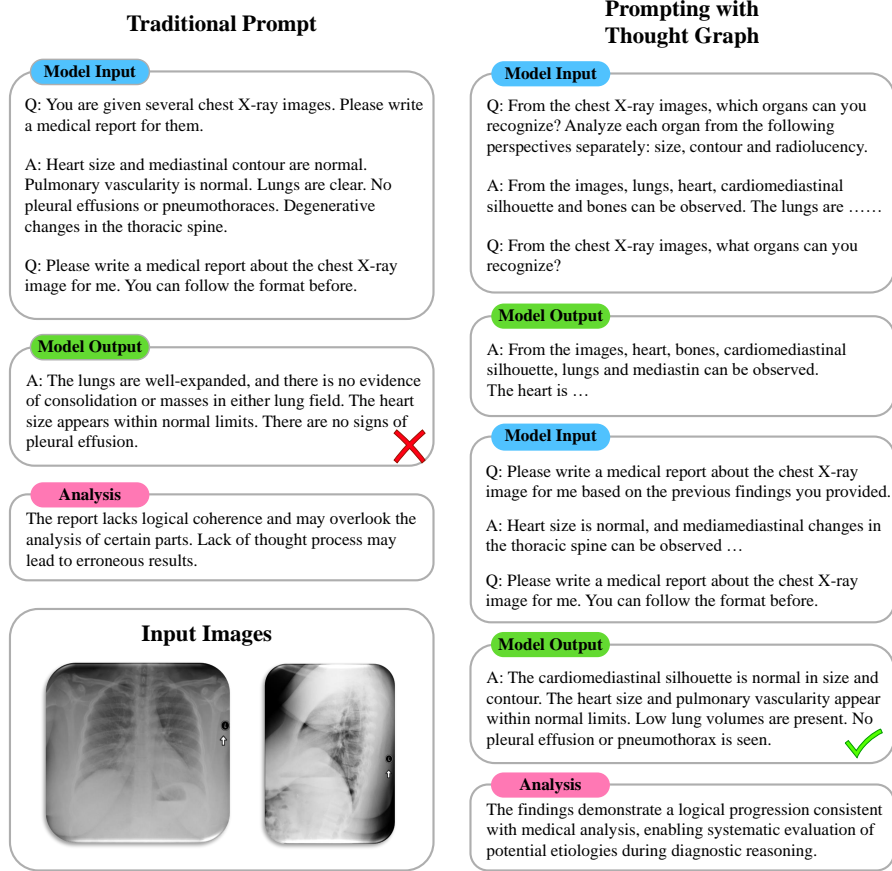


Figure 3: **Examples of conventional prompting and our Thought Graph.** (Left) Conventional prompting mimics stylistic examples without deep understanding, often leading to hallucinations or logically inconsistent reports. (Right) Our method explicitly guides the model’s attention toward organ-level reasoning and enforces a medically coherent reasoning order, leading to more accurate, logical, and interconnected diagnostic statements in the generated report.

insufficient pretraining on general-purpose reasoning tasks, prompt engineering has minimal effect on steering their output structure or depth of inference. Therefore, we do not rely on such architectures and instead build our framework on top of general-purpose, instruction-tuned large language models (*e.g.*, HuatuoGPT [30]) with strong multimodal alignment and reasoning ability, allowing for controllable, multi-step report generation at test time.

Addressing these limitations, we propose a approach that explicitly manages the depth of reasoning within VLLMs during inference, as depicted in Figure 2. We conduct extensive ablation experiments targeting the structured reasoning of VLLM’s results and test-time scaling. By integrating a dedicated reasoning mechanism, our model dynamically controls the extent of logical reasoning at test time, enabling deeper and more clinically relevant analyses. Additionally, we introduce a Thought Graph Traver-

---

**Algorithm 1** Thought Graph Traversal

---

**Require:** Patient X-ray images  $\{\mathbf{x}_i\}$ , Organ list  $\mathcal{O}$ , Expert database  $\mathcal{D}$ **Ensure:** Full medical report  $\mathbf{y}$ 

```
1: Initialize  $\mathbf{y} \leftarrow \emptyset$ 
2: for each organ  $o \in \mathcal{O}$  do
3:    $Q \leftarrow \text{GetQuestions}(o)$  ▷ Retrieve diagnostic questions
4:    $A \leftarrow \emptyset$ 
5:   for each question  $q \in Q$  do
6:      $Verified \leftarrow \text{False}$ 
7:     while not  $Verified$  do
8:        $a \leftarrow \text{VLM.Answer}(\{\mathbf{x}_i\}, q)$ 
9:        $Verified \leftarrow \text{VLM.Verify}(\{\mathbf{x}_i\}, q, a)$  ▷ Verification Step
10:    Append  $a$  to  $A$ 
11:    $\mathcal{E}_o \leftarrow \text{SampleExamples}(\mathcal{D}, o, k = 5)$  ▷ Few-shot ICL examples
12:    $r_o \leftarrow \text{VLM.GenerateReport}(\{\mathbf{x}_i\}, Q, A, \mathcal{E}_o)$ 
13:   Append  $r_o$  to  $\mathbf{y}$ 
14: return  $\mathbf{y}$ 
```

---

sal framework enriched with structured prior medical knowledge, systematically guiding the model towards logically coherent and medically accurate outputs. An additional benefit of this module is its capacity to expose underlying biases present in chest X-ray datasets, which is crucial for improving model generalizability and fairness.

Specifically, our method introduces: (1) A Thought Graph Traversal module that infuses structured medical knowledge  $\mathcal{K}$  to guide report generation. (2) A controllable reasoning mechanism, allowing dynamic adjustment of inference depth. With these components, our approach moves beyond surface-level generation and enables deeper, more interpretable, and more consistent diagnostic outputs.

### 3.2. Test-Time Reasoning via Graph Traversal

We classify our graph traversal into **1) Sequential traversal**, where later computations depend on earlier ones (*e.g.*, a long reasoning trace), and **2) Parallel traversal**, where computations run independently (*e.g.*, majority voting). We choose sequential scaling first as, intuitively, we believe it should scale better, since later computations can build on intermediate results, allowing for deeper reasoning and iterative refinement. We propose new sequential scaling methods and ways to benchmark them. Our main process for report generation is shown in Algorithm 1.

Our data consists of multiple X-ray images per patient as input  $\{\mathbf{x}_1, \dots, \mathbf{x}_n\}$  and a corresponding expert-written report  $\mathbf{y}$ , which includes several sentences, each describing a particular organ. The goal is to generate  $\mathbf{y}$  from the image set  $\{\mathbf{x}_i\}$  using a vision-language model.

Before prediction, we divide the dataset into a pseudo-training set and a pseudo-testing set. No VLM training is involved; instead, we use the training set to extract prior knowledge for structured reasoning. Specifically, we use GPT-4o to extract all

organ names mentioned in training reports:

$$\mathcal{O} = \{o_1, o_2, \dots, o_m\},$$

which are stored in an *organ list*. For each organ  $o_i$ , we store its associated textual descriptions from the training reports in a retrieval database. These organ-wise sentences serve as in-context learning (ICL) examples for later inference.

We formulate the structured report generation process as a reasoning traversal over a conceptual graph  $\mathcal{G}$ , where each node corresponds to an organ  $o \in \mathcal{O}$ , and each node branches into seven child nodes representing domain-specific diagnostic questions  $\mathcal{Q} = \{q_1, \dots, q_7\}$ .

*Graph Construction.* The graph  $\mathcal{G}$  is constructed as a two-level hierarchy:

- The root node corresponds to the entire patient case (*i.e.*,  $\{\mathbf{p}_i\}$ ).
- The first level consists of organ nodes  $\{o_1, o_2, \dots, o_m\}$  extracted from training data.
- Each organ node  $o$  connects to a fixed sequence of diagnostic question nodes  $\{q_1, \dots, q_7\}$ , forming a reasoning subgraph for that organ.

*Traversal Strategy.* During inference, we adopt a two-level traversal of the graph:

- Starting from the root, we iterate through all organ nodes  $o \in \mathcal{O}$  (*i.e.*, **in parallel** over organs).
- For each organ node, we expand all of its child question nodes  $\{q_1, \dots, q_7\}$  **in sequence**.
- Each question  $q_j$  is paired with the patient images  $\{\mathbf{x}_i\}$  and passed to the VLM to obtain an answer  $a_j$ :

$$a_j = \text{VLM.Answer}(\{\mathbf{x}_i\}, q_j), \quad j = 1, \dots, 7.$$

- After an initial answer  $a_j$  is generated, a verification step is performed to ensure its consistency with the question  $q_j$  and the input images  $\{\mathbf{x}_i\}$ :

$$\text{Verified} = \text{VLM.Verify}(\{\mathbf{x}_i\}, q_j, a_j)$$

If not verified, The VLM is continuously asked to re-generate its answer until verified.

- These  $(q_j, a_j)$  pairs form the reasoning context for generating an organ-specific report sentence  $s_o$ :

$$r_o = \text{VLM.GenerateReport}(\{\mathbf{x}_i\}, \{(q_j, a_j)\}_{j=1}^7, \mathcal{E}_o),$$

where  $\mathcal{E}_o$  denotes retrieved in-context examples from the training corpus.



*Report Assembly.* The final report  $\mathbf{y}$  is obtained by sequentially concatenating the generated descriptions  $r_o$  in the original organ order:

$$\mathbf{y} = [r_{o_1}, r_{o_2}, \dots, r_{o_m}].$$

This structured and graph-aware design offers several key benefits: **Scalability:** Each organ’s reasoning process is modular, allowing parallel execution and easy extension to more question types or organs. **Interpretability:** The BFS-style traversal mirrors clinical workflows and enables introspection into intermediate reasoning steps. **Controllability:** The system allows flexible prompt-level manipulation, such as adjusting question depth, skipping irrelevant organs, or pruning low-confidence answers.

### 3.3. Budget Forcing via Iterative Traversal

Building on the graph-based reasoning framework in Section 3.2, we further introduce a **budget forcing** mechanism to regulate the amount of computation during test-time traversal. While Section 3.2 adopts a parallel-sequence framework over the structured reasoning graph  $\mathcal{G}$  to cover all diagnostic questions per organ, here we refine that process by limiting how deep or how far the traversal proceeds, *i.e.*, how many reasoning tokens the model is allowed to consume.

Instead of generating all question-answer pairs in a single pass, we initiate a multi-round inference process. In each round, follow-up questions are asked based on prior responses, aiming to explore new diagnostic angles and progressively deepen reasoning. This iterative reasoning is still rooted in the BFS-style traversal introduced earlier but adds a temporal dimension: each organ node now accumulates its subgraph traversal over time, guided by token budget constraints.

As illustrated in Figure 1, we observe a clear positive correlation between the number of reasoning tokens and report quality. However, model performance plateaus around 450 tokens, indicating that additional reasoning beyond this point yields minimal improvement. This saturation point provides a practical guideline for balancing inference cost and quality under test-time compute constraints.

To further ensure the reliability of the generated content, we introduce a final verification step. After producing an initial sentence  $s_o$  for each organ, the VLM revisits the reasoning path taken (*i.e.*, the sequence of  $(q_j, a_j)$  pairs) and evaluates whether the generated output is coherent and justified. If inconsistencies are detected—such as unsupported conclusions or logical contradictions—the system re-enters the reasoning loop for that organ, repeating the traversal with updated prompts until a satisfactory report is obtained.

## 4. Experiments

### 4.1. Datasets and Metrics

IU X-Ray [33] is a widely used publicly available dataset for medical report generation tasks containing 3,955 fully de-identified radiology reports with sections such as Impression, Findings, Indication, etc., each associated with frontal and/or lateral chest X-rays, totaling 7,470 images.

Table 1: **Comparison of Zero-Shot, traditional Few-Shot, and Thought Graph Traversal on the IU X-Ray dataset.** The table reports evaluation metrics including BLEU-1 to BLEU-4, METEOR, and ROUGE-L across three models (GPT-4o [30], Qwen2.5-VL [31], and HuatuoGPT-Vision [32]). Thought graph traversal (TGT) consistently achieves higher scores, indicating improved report generation quality.

		BLEU-1	BLEU-2	BLEU-3	BLEU-4	METEOR	ROUGE-L
GPT-4o	Zero-Shot	17.72	7.02	11.20	7.24	18.94	26.87
	Few-Shot	35.90	18.91	13.38	8.42	20.62	29.40
	TGT	<b>40.41</b>	<b>27.31</b>	<b>18.62</b>	<b>12.16</b>	<b>20.93</b>	<b>35.95</b>
Qwen2.5-VL	Zero-Shot	17.74	7.00	10.16	6.22	18.96	16.83
	Few-Shot	29.84	18.89	12.35	10.39	19.18	29.30
	TGT	<b>38.95</b>	<b>25.85</b>	<b>18.36</b>	<b>12.03</b>	<b>19.29</b>	<b>36.12</b>
HuatuoGPT-Vision	Zero-Shot	14.74	5.99	2.77	1.14	15.75	14.01
	Few-Shot	33.91	23.68	11.99	9.90	20.94	25.02
	TGT	<b>43.46</b>	<b>28.85</b>	<b>19.10</b>	<b>12.14</b>	<b>21.77</b>	<b>37.33</b>

Table 2: **Comparison of Zero-Shot, traditional Few-Shot, and Thought Graph Traversal prompting on the MIMIC-CXR dataset.** The table reports evaluation metrics including BLEU-1 to BLEU-4, METEOR, and ROUGE-L across three models (GPT-4o, Qwen2.5-VL, and HuatuoGPT-Vision). Values are presented in percentage (%). Thought graph traversal consistently achieves higher scores, indicating improved report generation quality.

		BLEU-1	BLEU-2	BLEU-3	BLEU-4	METEOR	ROUGE-L
GPT-4o	Zero-Shot	19.01	5.61	1.42	1.03	12.40	16.27
	Few-Shot	24.89	11.85	4.31	5.18	12.94	22.28
	TGT	<b>29.25</b>	<b>15.81</b>	<b>8.95</b>	<b>9.84</b>	<b>14.12</b>	<b>26.50</b>
Qwen2.5-VL	Zero-Shot	20.23	5.36	1.48	1.14	11.30	14.64
	Few-Shot	22.58	9.39	3.40	5.41	13.65	15.63
	TGT	<b>26.33</b>	<b>14.78</b>	<b>8.35</b>	<b>8.82</b>	<b>13.78</b>	<b>24.34</b>
HuatuoGPT-Vision	Zero-Shot	24.81	7.92	2.45	1.24	10.18	17.76
	Few-Shot	27.82	14.50	6.75	6.61	13.61	18.10
	TGT	<b>32.99</b>	<b>18.89</b>	<b>10.85</b>	<b>11.34</b>	<b>14.36</b>	<b>27.06</b>

MIMIC-CXR [34] is currently the largest public dataset containing many chest radiograph images and reports. In total, this dataset has 377,110 images and 227,835 reports for 64,588 patients. For experimental and fair comparisons, we followed the previous methodology [19] used the official MIMIC-CXR divisions: 222,758 samples for training, 1,808 for validation, and 3,269 for testing.

We evaluated radiology report generation using standard natural language generation (NLG) metrics. The NLG metrics were BLEU [35], METEOR [36], and ROUGE [37] scores, which are standard metrics used to assess the fluency of generated natural language.

#### 4.2. Results

**Thought graph traversal enhances reasoning depth and report quality up to a threshold.** We explore the effect of structured question prompting on reasoning depth. By controlling the number of diagnostic questions asked prior to report generation, we indirectly modulate the model’s token budget for reasoning. As Figure 1 demonstrates, increasing the number of targeted diagnostic queries leads to higher report quality up to a threshold (4 queries), beyond which marginal gains plateau. This suggests that early reasoning steps already address core findings, and later queries add limited value due to informational redundancy.

**Compared to no prompting, our Thought Graph Traversal method introduces structured reasoning that significantly improves report completeness and medical**

Table 3: **Comparison of different prompting or scaling strategies, including RaR [38], On-MP [39], and Self-Refine [40], for HuatuoGPT on the IU X-Ray dataset.** Metrics include BLEU-1 to BLEU-4, METEOR, and ROUGE-L. Thought graph traversal achieves the best overall performance. Values are presented in percentage (%).

Method	BLEU-1	BLEU-2	BLEU-3	BLEU-4	METEOR	ROUGE-L
RaR [38]	26.22	11.58	6.36	3.25	14.58	17.74
On-MP [39]	20.74	8.81	4.38	2.25	13.79	20.38
Self-Refine [40]	18.72	8.58	4.44	2.28	15.41	19.47
TGT	<b>43.46</b>	<b>28.85</b>	<b>19.10</b>	<b>12.14</b>	<b>21.77</b>	<b>37.33</b>

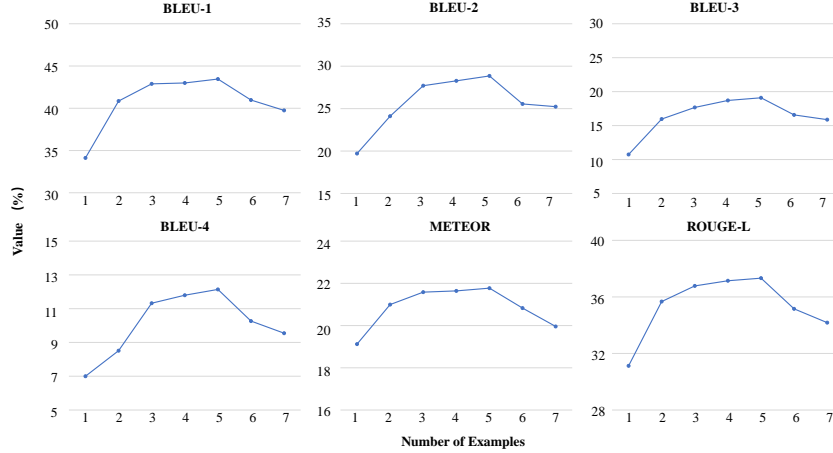


Figure 4: **Impact of example quantity in prompt design.** We empirically study the effect of example count on model performance during chest X-ray report generation. Using our curated prompt with seven examples as a baseline, we observe that reducing the number of examples significantly degrades report quality due to insufficient guidance, leading to reasoning and formatting errors. Interestingly, increasing the number of examples beyond five also causes a performance drop. This is likely due to the model overfitting to the examples, prioritizing mimicking their patterns over analyzing the actual image, or being misled by repeated or similar examples, thereby reducing factual accuracy.

**accuracy.** Shown in Table 1, Table 2, without any prompt guidance, vision-language models often rely solely on their pretrained biases, leading to generic, underspecified, or irrelevant reports. Thought graph traversal provides a scaffolded inference process by decomposing the task into organ-wise diagnostic reasoning steps, prompting the model to attend to clinically meaningful visual patterns. For example, on the MIMIC-CXR dataset, GPT-4o’s BLEU-4 score improves from **1.03 (Zero-Shot)** to **9.84 (Thought Graph Traversal)**; similarly, HuatuoGPT-Vision improves from **1.24 to 11.34**, showing substantial gains in output specificity and image-grounding (Table 2).

**Compared to conventional prompt engineering, Thought Graph Traversal further enhances factual accuracy and logical consistency.** As illustrated in Figure 3, traditional few-shot prompting—focused on mimicking the format and wording of examples—often causes imitation bias, leading to hallucinated findings and anatomically implausible statements. In contrast, Thought Graph Traversal explicitly guides

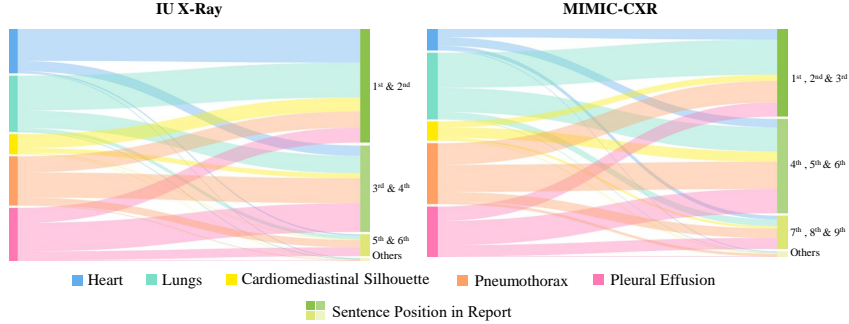


Figure 5: **Analysis of organ description positions in expert-written reports from the IU X-Ray and MIMIC-CXR datasets.** The left y-axis represents the different organs, and the right y-axis indicates the sentence number in the report where each organ is mentioned. The figure shows that certain organs, such as the heart and lungs, tend to appear earlier in reports, while pathological findings are more commonly placed later. This positional pattern suggests that organ-level descriptions follow a latent structural order. To quantify this, we prompt GPT-4o to extract organ-related sentences from each report and pair them with their corresponding organs. These organ-sentence pairs are stored in structured resources (`organ_list`, `database`), enabling visualization and modeling of organ-specific sentence distribution.

the model in analyzing the image organ by organ, with each reasoning step informed by representative examples and structured medical knowledge. For instance, HuatuoGPT with Thought Graph Traversal achieves a BLEU-4 score of **12.14**, outperforming **RaR (3.25)**, **On-MP (2.25)**, and **Self-Refine (2.28)** by large margins across all evaluation metrics (Table 3).

**Increasing ICL examples improves performance up to a point.** To understand the role of in-context learning (ICL) scale, we vary the number of examples in the prompt. As shown in Figure 4, performance improves when increasing the number of examples from 1 to 5, but begins to decline beyond 5. We attribute this to cognitive overload: when too many examples are included, the model’s attention shifts from visual grounding to excessive example matching, causing reduced clinical validity and misprioritized findings.

**Dataset bias on organ description order.** Moreover, our analysis of expert reports reveals a consistent positional bias in organ descriptions. For example, heart and lung findings are frequently mentioned at the beginning of a report, while soft tissue or osseous findings appear later. To leverage this, we use GPT-4o to extract organ-mention pairs from reports, organizing them into an `organ_list` and `database`. This structure supports a report generation sequence that mirrors expert writing patterns, as shown in Figure 5.

To quantitatively assess the impact of organ description order on report quality, we conducted a controlled experiment in which all other prompting variables were held constant, and only the order of organ reasoning steps in the graph was varied. Specifically, we tested all possible permutations of the five organs involved in the Thought Graph Traversal graph (*i.e.*,  $5! = 120$  permutations). For each permutation, we evaluated the resulting report using six metrics: BLEU-1 through BLEU-4, METEOR, and ROUGE-L.

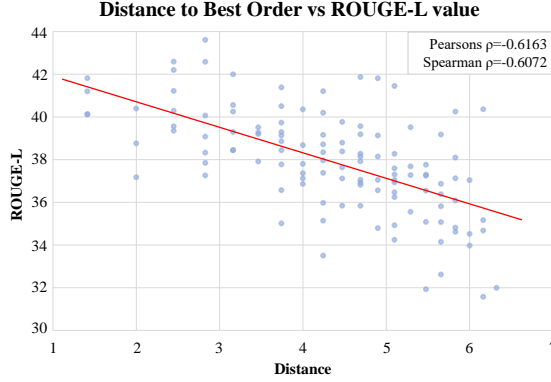


Figure 6: **The scatter plot showing the relationship between organ order distance and the ROUGE-L values.** We conduct experiment across all 120 permutations of five organs in the reasoning graph. Correlation analysis reveals that ROUGE-L is sensitive to organ sequence, with statistically significant negative correlations (Spearman  $\rho = -0.6163$ ,  $p = 8.53 \times 10^{-14}$ ; Pearson  $\rho = -0.6072$ ,  $p = 2.45 \times 10^{-13}$ ), suggesting the importance of logical ordering in radiology report generation.

Let  $\text{ord}_i \in \mathbb{N}^5$  denote the  $i$ -th permutation of organ order, and let  $\text{metric}_{k,i} \in \mathbb{R}_+$  be the corresponding evaluation score for metric  $k$  ( $k = 1, \dots, 6$ ). For each metric  $k$ , we first identify the index  $i_k^*$  that yields the highest score, defined as  $i_k^* = \arg \max_i \text{metric}_{k,i}$ . The permutation corresponding to this index,  $\mathbf{b}_k = \text{ord}_{i_k^*}$ , is defined as the best organ order for metric  $k$ . Then, for each permutation  $i$ , we compute its Euclidean distance to the best order:

$$x_{k,i} = \sqrt{\sum_{j=1}^5 (\text{ord}_{i,j} - \mathbf{b}_{k,j})^2},$$

and plot  $x_{k,i}$  (organ order distance) against  $\text{metric}_{k,i}$  (performance) to examine the sensitivity of each metric to organ ordering.

We perform both Spearman and Pearson correlation tests to assess statistical dependence. The results show that ROUGE-L is notably sensitive to organ ordering, with a Spearman correlation of  $-0.6163$  ( $p = 8.53 \times 10^{-14}$ ) and a Pearson correlation of  $-0.6072$  ( $p = 2.45 \times 10^{-13}$ ), as shown in Figure 6. This suggests that coherent sequencing of organ descriptions strongly affects linguistic overlap with ground-truth reports and highlights the importance of order modeling in structured report generation.

## 5. Conclusion

In this work, we present a test-time scaling framework for chest X-ray report generation that addresses the limitations of shallow reasoning in existing VLLM-based approaches. By introducing a controllable reasoning mechanism and integrating structured medical priors through a Thought Graph Traversal, our method enables stepwise, organ-aware analysis that enhances both the logical consistency and diagnostic correctness of generated reports. Extensive experiments on IU X-Ray and MIMIC-CXR

demonstrate that our model significantly outperforms traditional zero-shot and few-shot baselines across multiple evaluation metrics. Ablation studies further confirm the importance of reasoning depth, prompt structure, and organ ordering in improving generation quality. Notably, we show that the order in which organs are analyzed affects model performance, and that optimizing this order can lead to statistically significant gains, especially in metrics like ROUGE-L. Our findings highlight the importance of structured, interpretable reasoning in medical report generation and suggest new directions for controlling inference dynamics in large medical VLLMs.

## References

- [1] J. Hoffmann, S. Borgeaud, A. Mensch, E. Buchatskaya, T. Cai, E. Rutherford, D. de Las Casas, L. A. Hendricks, J. Welbl, A. Clark, et al., Training compute-optimal large language models, in: *Proceedings of the 36th International Conference on Neural Information Processing Systems*, 2022, pp. 30016–30030.
- [2] N. Muennighoff, Z. Yang, W. Shi, X. L. Li, L. Fei-Fei, H. Hajishirzi, L. Zettlemoyer, P. Liang, E. Candès, T. Hashimoto, s1: Simple test-time scaling, *arXiv preprint arXiv:2501.19393* (2025).
- [3] F. Wang, Z. Han, X. Liu, Y. Yin, X. Gao, Ctpt: Continual test-time prompt tuning for vision-language models, *Pattern Recognition* 161 (2025) 111300.
- [4] J. Yin, X. Zhang, L. Wu, X. Wang, Context-aware prompt learning for test-time vision recognition with frozen vision-language model, *Pattern Recognition* (2025) 111359.
- [5] C. Snell, J. Lee, K. Xu, A. Kumar, *Scaling llm test-time compute optimally can be more effective than scaling model parameters* (2024). *arXiv:2408.03314*. URL <https://arxiv.org/abs/2408.03314>
- [6] OpenAI, *Learning to reason with llms* (September 2024). URL <https://openai.com/index/learning-to-reason-with-llms/>
- [7] Y. Zhang, S. Wu, Y. Yang, J. Shu, J. Xiao, C. Kong, J. Sang, *o1-coder: an o1 replication for coding* (2024). *arXiv:2412.00154*. URL <https://arxiv.org/abs/2412.00154>
- [8] Y. Qin, X. Li, H. Zou, Y. Liu, S. Xia, Z. Huang, Y. Ye, W. Yuan, H. Liu, Y. Li, P. Liu, *O1 replication journey: A strategic progress report – part 1* (2024). *arXiv:2410.18982*. URL <https://arxiv.org/abs/2410.18982>
- [9] DeepSeek-AI, *Deepseek-rl: Incentivizing reasoning capability in llms via reinforcement learning* (2025). *arXiv:2501.12948*. URL <https://arxiv.org/abs/2501.12948>
- [10] Z. Chen, Y. Song, T.-H. Chang, X. Wan, Generating radiology reports via memory-driven transformer, in: *Proceedings of the 2020 Conference on Empirical Methods in Natural Language Processing (EMNLP)*, 2020, pp. 1439–1449.

- [11] D. Ganeshan, P.-A. T. Duong, L. Probyn, L. Lenchik, T. A. McArthur, M. Retrouvey, E. H. Ghobadi, S. L. Desouches, D. Pastel, I. R. Francis, Structured reporting in radiology, *Academic radiology* 25 (1) (2018) 66–73.
- [12] T. Miller, Explanation in artificial intelligence: Insights from the social sciences, *Artificial intelligence* 267 (2019) 1–38.
- [13] OpenAI, J. Achiam, S. Adler, S. Agarwal, L. Ahmad, I. Akkaya, F. L. Aleman, D. Almeida, J. Altenschmidt, S. Altman, et al., Gpt-4 technical report (2023). [arXiv:2303.08774](https://arxiv.org/abs/2303.08774).
- [14] A. Radford, J. W. Kim, C. Hallacy, A. Ramesh, G. Goh, S. Agarwal, G. Sastry, A. Askell, P. Mishkin, J. Clark, et al., Learning transferable visual models from natural language supervision, in: *International conference on machine learning*, PMLR, 2021, pp. 8748–8763.
- [15] C. Wu, S. Yin, W. Qi, X. Wang, Z. Tang, N. Duan, Visual chatgpt: Talking, drawing and editing with visual foundation models, *arXiv preprint arXiv:2303.04671* (2023).
- [16] Z. Wang, L. Liu, L. Wang, L. Zhou, Metransformer: Radiology report generation by transformer with multiple learnable expert tokens, in: *Proceedings of the IEEE/CVF Conference on Computer Vision and Pattern Recognition*, 2023, pp. 11558–11567.
- [17] S. Yang, X. Wu, S. Ge, Z. Zheng, S. K. Zhou, L. Xiao, Radiology report generation with a learned knowledge base and multi-modal alignment, *Medical Image Analysis* 86 (2023) 102798.
- [18] T. Tanida, P. Müller, G. Kaissis, D. Rueckert, Interactive and explainable region-guided radiology report generation, in: *Proceedings of the IEEE/CVF Conference on Computer Vision and Pattern Recognition*, 2023, pp. 7433–7442.
- [19] H. Qin, Y. Song, Reinforced cross-modal alignment for radiology report generation, in: *Findings of the Association for Computational Linguistics: ACL 2022*, 2022, pp. 448–458.
- [20] F. Liu, X. Wu, S. Ge, W. Fan, Y. Zou, Exploring and distilling posterior and prior knowledge for radiology report generation, in: *Proceedings of the IEEE/CVF conference on computer vision and pattern recognition*, 2021, pp. 13753–13762.
- [21] M. Li, B. Lin, Z. Chen, H. Lin, X. Liang, X. Chang, Dynamic graph enhanced contrastive learning for chest x-ray report generation, in: *Proceedings of the IEEE/CVF Conference on Computer Vision and Pattern Recognition*, 2023, pp. 3334–3343.
- [22] Z. Huang, X. Zhang, S. Zhang, Kiut: Knowledge-injected u-transformer for radiology report generation, in: *Proceedings of the IEEE/CVF Conference on Computer Vision and Pattern Recognition*, 2023, pp. 19809–19818.

- [23] T. Brown, B. Mann, N. Ryder, M. Subbiah, J. D. Kaplan, P. Dhariwal, A. Nee-lakantan, P. Shyam, G. Sastry, A. Askell, et al., Language models are few-shot learners, *Advances in neural information processing systems* 33 (2020) 1877–1901.
- [24] J. Wei, X. Wang, D. Schuurmans, M. Bosma, F. Xia, E. Chi, Q. V. Le, D. Zhou, et al., Chain-of-thought prompting elicits reasoning in large language models, *Advances in neural information processing systems* 35 (2022) 24824–24837.
- [25] T. Kojima, S. S. Gu, M. Reid, Y. Matsuo, Y. Iwasawa, Large language models are zero-shot reasoners, in: *Advances in Neural Information Processing Systems*, 2022.
- [26] Y. Liu, J. Singh, G. Liu, A. Payani, L. Zheng, Towards hierarchical multi-agent workflows for zero-shot prompt optimization, *arXiv preprint arXiv:2405.20252* (2024).
- [27] Z. Hu, P. Yang, Y. Jiang, Z. Bai, Prompting large language model with context and pre-answer for knowledge-based vqa, *Pattern Recognition* 151 (2024) 110399.
- [28] S. Yao, D. Yu, J. Zhao, I. Shafran, T. Griffiths, Y. Cao, K. Narasimhan, *Tree of thoughts: Deliberate problem solving with large language models*, in: A. Oh, T. Naumann, A. Globerson, K. Saenko, M. Hardt, S. Levine (Eds.), *Advances in Neural Information Processing Systems*, Vol. 36, Curran Associates, Inc., 2023, pp. 11809–11822.  
URL [https://proceedings.neurips.cc/paper\\_files/paper/2023/file/271db9922b8d1f4dd7aaef84ed5ac703-Paper-Conference.pdf](https://proceedings.neurips.cc/paper_files/paper/2023/file/271db9922b8d1f4dd7aaef84ed5ac703-Paper-Conference.pdf)
- [29] Z. Gou, Z. Shao, Y. Gong, Y. Shen, Y. Yang, N. Duan, W. Chen, *Critic: Large language models can self-correct with tool-interactive critiquing* (2024). *arXiv: 2305.11738*.  
URL <https://arxiv.org/abs/2305.11738>
- [30] J. Chen, C. Gui, R. Ouyang, A. Gao, S. Chen, G. H. Chen, X. Wang, R. Zhang, Z. Cai, K. Ji, G. Yu, X. Wan, B. Wang, *Huatuogpt-vision, towards injecting medical visual knowledge into multimodal llms at scale* (2024). *arXiv: 2406.19280*.  
URL <https://arxiv.org/abs/2406.19280>
- [31] S. Bai, K. Chen, X. Liu, J. Wang, W. Ge, S. Song, K. Dang, P. Wang, S. Wang, J. Tang, H. Zhong, Y. Zhu, M. Yang, Z. Li, J. Wan, P. Wang, W. Ding, Z. Fu, Y. Xu, J. Ye, X. Zhang, T. Xie, Z. Cheng, H. Zhang, Z. Yang, H. Xu, J. Lin, *Qwen2.5-vl technical report* (2025). *arXiv:2502.13923*.  
URL <https://arxiv.org/abs/2502.13923>
- [32] OpenAI, *Gpt-4o system card* (2024). *arXiv:2410.21276*.  
URL <https://arxiv.org/abs/2410.21276>
- [33] J. Pavlopoulos, V. Kougia, I. Androutsopoulos, A survey on biomedical image captioning, in: *Proceedings of the second workshop on shortcomings in vision and language*, 2019, pp. 26–36.



- [34] A. E. Johnson, T. J. Pollard, N. R. Greenbaum, M. P. Lungren, C.-y. Deng, Y. Peng, Z. Lu, R. G. Mark, S. J. Berkowitz, S. Horng, Mimic-cxr-jpg, a large publicly available database of labeled chest radiographs, arXiv preprint arXiv:1901.07042 (2019).
- [35] K. Papineni, S. Roukos, T. Ward, W.-J. Zhu, Bleu: a method for automatic evaluation of machine translation, in: Proceedings of the 40th annual meeting of the Association for Computational Linguistics, 2002, pp. 311–318.
- [36] S. Banerjee, A. Lavie, Meteor: An automatic metric for mt evaluation with improved correlation with human judgments, in: Proceedings of the acl workshop on intrinsic and extrinsic evaluation measures for machine translation and/or summarization, 2005, pp. 65–72.
- [37] C.-Y. Lin, Rouge: A package for automatic evaluation of summaries, in: Text summarization branches out, 2004, pp. 74–81.
- [38] Y. Deng, W. Zhang, Z. Chen, Q. Gu, Rephrase and respond: Let large language models ask better questions for themselves, arXiv preprint arXiv:2311.04205 (2023).
- [39] A. de Wynter, X. Wang, Q. Gu, S.-Q. Chen, On meta-prompting, arXiv preprint arXiv:2312.06562 (2023).
- [40] A. Madaan, N. Tandon, P. Gupta, S. Hallinan, L. Gao, S. Wiegrefe, U. Alon, N. Dziri, S. Prabhunoye, Y. Yang, S. Gupta, B. P. Majumder, K. Hermann, S. Welleck, A. Yazdanbakhsh, P. Clark, [Self-refine: Iterative refinement with self-feedback](https://proceedings.neurips.cc/paper_files/paper/2023/file/91edff07232fb1b55a505a9e9f6c0ff3-Paper-Conference.pdf), in: A. Oh, T. Naumann, A. Globerson, K. Saenko, M. Hardt, S. Levine (Eds.), Advances in Neural Information Processing Systems, Vol. 36, Curran Associates, Inc., 2023, pp. 46534–46594.  
URL [https://proceedings.neurips.cc/paper\\_files/paper/2023/file/91edff07232fb1b55a505a9e9f6c0ff3-Paper-Conference.pdf](https://proceedings.neurips.cc/paper_files/paper/2023/file/91edff07232fb1b55a505a9e9f6c0ff3-Paper-Conference.pdf)